Original Article

Cytogenetic and Genome Research

Cytogenet Genome Res 2011;134:220–228
DOI: 10.1159/000327713

Accepted: February 28, 2011
by B. Friebe
Published online: May 3, 2011

Holocentric Chromosomes of *Luzula elegans* Are Characterized by a Longitudinal Centromere Groove, Chromosome Bending, and a Terminal Nucleolus Organizer Region

S. Heckmann[a] E. Schroeder-Reiter[b] K. Kumke[a] L. Ma[a] K. Nagaki[c]
M. Murata[c] G. Wanner[b] A. Houben[a]

[a]Leibniz Institute of Plant Genetics and Crop Plant Research (IPK), Gatersleben, and [b]Department of Biology I, Biocenter, Ludwig-Maximilians-University Munich, Planegg-Martinsried, Germany; [c]Institute of Plant Science and Resources, Okayama University, Kurashiki, Japan

Key Words
CENH3 · Centromere · Holocentric chromosome · *Luzula elegans* · Mitosis · rDNA

Abstract
The structure of holocentric chromosomes was analyzed in mitotic cells of *Luzula elegans*. Light and scanning electron microscopy observations provided evidence for the existence of a longitudinal groove along each sister chromatid. The centromere-specific histone H3 variant, CENH3, colocalized with this groove and with microtubule attachment sites. The terminal chromosomal regions were CENH3-negative. During metaphase to anaphase transition, *L. elegans* chromosomes typically curved to a sickle-like shape, a process that is likely to be influenced by the pulling forces of microtubules along the holocentric axis towards the corresponding microtubule organizing regions. A single pair of 45S rDNA sites, situated distal to *Arabidopsis*-telomere repeats, was observed at the terminal region of one chromosome pair. We suggest that the 45S rDNA position in distal centromere-free regions could be required to ensure chromosome stability.

A centromere is a specialized chromosomal region, where transiently a multi-protein complex, the kinetochore, assembles to which the spindle microtubules attach. Proper spindle microtubule attachment ensures faithful transmission of one sister chromatid to each daughter cell during mitosis. Establishment of active centromeres and their maintenance is primarily defined epigenetically by the incorporation of the centromere-specific histone H3 variant CENH3, originally termed CENP-A (mammalian centromere protein A) [Earnshaw and Rothfield, 1985], into centromeric nucleosomes [for review see Allshire and Karpen, 2008].

Most organisms feature one single size-restricted centromere per chromosome, referred to as monocentric chromosomes. However, in different independent eukaryotic lineages, including some green algae, various protozoa, many different invertebrate taxa, and plants, so-called holocentric chromosomes are found, suggesting that the phenomenon of holocentricity has arisen several times via convergent evolution [for reviews see Pimpinelli and Goday, 1989; Dernburg, 2001]. Holocentric chromosomes have no distinct primary constriction visible at metaphase, and spindle fibers are attached along almost the entire (Greek: holo-) poleward surface of the

KARGER
Fax +41 61 306 12 34
E-Mail karger@karger.ch
www.karger.com

1424–8581/11/1343–0220$38.00/0

Accessible online at:
www.karger.com/cgr

Andreas Houben
Leibniz Institute of Plant Genetics and Crop Plant Research (IPK)
Corrensstrasse 3
DE–06466 Gatersleben (Germany)
Tel. +49 39482 5486, E-Mail houben@ipk-gatersleben.de

chromatids. As a result, the sister chromatids migrate to opposite poles parallel to each other during anaphase, while in monocentric chromosomes microtubule spindles attach to a distinct kinetochore and the sister chromatids move to the poles at anaphase with the centromere leading [for review Guerra et al., 2010].

Based on our current knowledge and despite this cytologically distinct chromosomal architecture, the composition and the formation of kinetochores seem to be similar to those in monocentric chromosomes. The kinetochore proteins of active centromeres are similar in monocentric and holocentric chromosome species, suggesting that they use similar mechanisms to conduct mitotic chromosome segregation [Albertson and Thomson, 1982; Howe et al., 2001; Maddox et al., 2004; Nagaki et al., 2005; Oegema and Hyman, 2006; Kitagawa, 2009].

In *Caenorhabditis elegans* and *Luzula nivea* CENH3 localizes along mitotic chromosomes and correlates with active centromeres as in monocentric species [Buchwitz et al., 1999; Nagaki et al., 2005]. At metaphase, kinetochores of holocentric chromosomes appear as an almost continuous axial line in light microscopy, with exception of distal CENH3-free regions [Buchwitz et al., 1999; Moore et al., 1999; Nagaki et al., 2005]. However, in interphase and early mitotic stages, CENH3 signals are dispersed, forming various small foci in *L. nivea* and *C. elegans* [Moore et al., 1999; Nagaki et al., 2005].

Recently, Nagaki et al. [2005] noted that in the holocentric Juncaceae *L. nivea* the chromosomal regions colocalizing with CENH3 may be characterized by a groove-like structure. They proposed a centromere extension mechanism accounting for the formation of an outer groove along each chromatid. In order to examine whether a groove might be better visible in larger holocentric chromosomes, we selected *L. elegans* because of its large chromosomes for studies of the mitotic behavior and the structure of holocentric chromosomes.

Materials and Methods

Plant Material

The wood-rush *Luzula elegans* (2n = 6) and *L. luzuloides* (2n = 12) were used for the following experiments.

Chromosome Preparation for Fluorescence Light Microscopy

Mitotic chromosomes were prepared from flower buds or apical meristems, which were fixed 45 min with ice-cold 4% paraformaldehyde in MTSB buffer (50 mM PIPES, 5 mM $MgSO_4$, and 5 mM EGTA, pH 7.2). After washing in MTSB, chromosome spreads were prepared by squashing, and coverslips were removed after freezing in liquid nitrogen.

Immunostaining was performed as described [Houben et al., 2007]. A rabbit anti-LnCENH3 antibody (1:100) [Nagaki et al., 2005] together with a mouse anti-α-tubulin monoclonal antibody (1:200) (clone DM 1A, Sigma) were applied as primary antibodies, and a Cy3-conjugated anti-rabbit IgG (1:500) (Dianova) and a FITC-conjugated anti-mouse Alexa 488 antibody (1:500) (Molecular Probes) were used as secondary antibodies.

Immunofluorescence images were recorded with an Olympus BX61 microscope equipped with an ORCA-ER CCD camera (Hamamatsu). Deconvolution microscopy was employed for superior optical resolution of globular structures. Thus, each photograph was collected as a sequential image along the Z-axis with approximately 11 slices per specimen. All images were collected in grey scale and pseudocolored with Adobe Photoshop. Projections (maximum intensity) and picture tilts were done with the program AnalySIS (Soft Imaging System).

Probe Preparation and Fluorescence in situ Hybridization

Nuclear 45S ribosomal DNA was probed using the clone pTa71 [Gerlach and Bedbrook, 1979], and telomeric DNA was detected using PCR-generated *Arabidopsis*-type repeats according to Cox et al. [1993]. DNA probes were directly labeled by nick translation with Cy5-dUTP and Alexa 488-dUTP according to Kato et al. [2006].

Chromosome spreads were prepared from ethanol:acetic acid (3:1)-fixed flower buds or apical meristems. After dehydration of spreads, the specimens were cross-linked using a UV-light illuminator, and the FISH procedure was employed according to Mandakova and Lysak [2008]. Chromosomes were subsequently treated with 45% acetic acid for 10 min at room temperature and with pepsin (0.1 mg/ml in 0.01 N HCl) for 10 min at 37°C, post-fixed in 2.5% formaldehyde in 2× SSC for 6 min, dehydrated in an ethanol series, and air dried. The hybridization mixture (50% formamide and 10% dextran sulfate in 2× SSC) containing the probe was denatured together with the chromosomal DNA on a heating plate at 80°C for 5 min and hybridized at 37°C overnight. Post-hybridization washing was carried out in 2× SSC for 20 min at 57°C. After dehydration, the slides were counterstained with 4′,6-diamidino-2-phenylindole (DAPI) in Vectashield (Vector Laboratories). Fluorescence pictures were taken as described above.

Scanning Electron Microscopy

For scanning electron microscopy investigations (SEM), root tips from cultivated plants were harvested, fixed in ethanol:acetic acid (3:1) and stored at least 12 h at –20°C. Chromosomes were isolated, dropped onto laser-marked glass slides (LaserMarking), and fixed in glutardialdehyde (2.5% in 75 mM cacodylate buffer, pH 7.0) according to the drop/cryo technique [Martin et al., 1994]. For DNA staining, chromosomes were dropped onto carbon-coated slides, incubated for 30 min at room temperature with Platinum Blue (5 mM $[CH_3CN]_2Pt$ oligomer in 75 mM cacodylate buffer, pH 7.0), and subsequently washed with buffer and distilled water [Wanner and Formanek, 1995]. Prior to SEM, specimens were dehydrated in 100% acetone, critical point dried from CO_2, cut to size, and mounted onto aluminum stubs with carbon conductive adhesive (Plano). Specimens were sputter-coated to 2 nm with platinum (BAE S050, Balzers) and examined at 0.7–1.5 kV with a Zeiss Auriga field emission scanning electron microscope (FESEM) equipped with a chamber Everhard-Thorn-

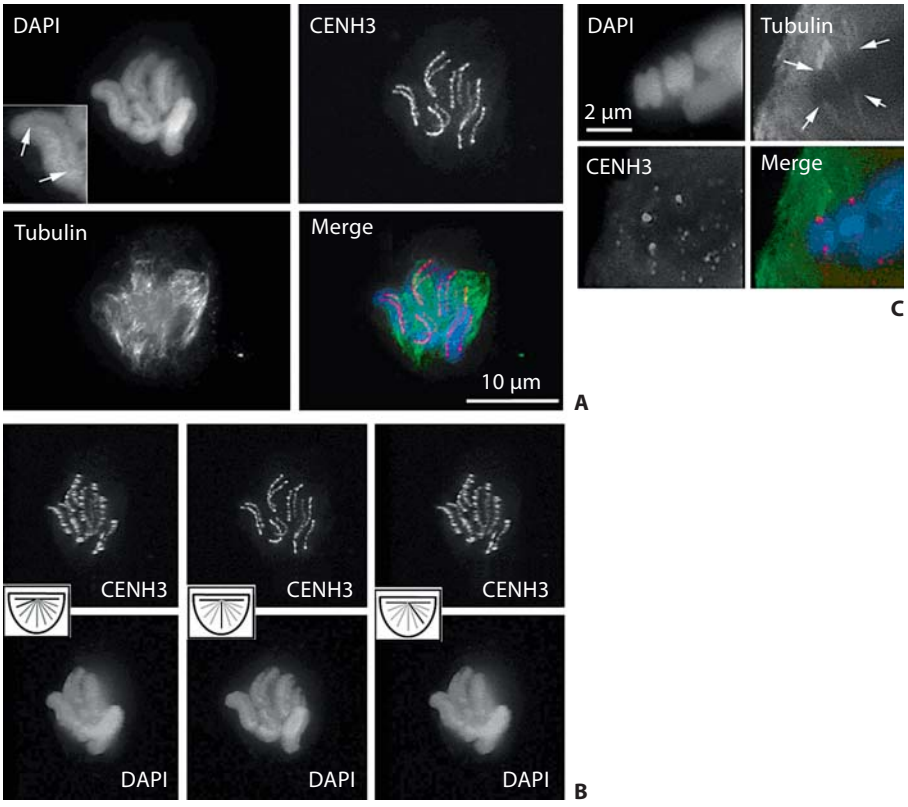

Fig. 1. Fluorescence light microscopy of mitotic metaphase chromosomes of *L. elegans*. DAPI-stained chromosomes are blue, CENH3 signals are red, and α-tubulin is green. **A** Immunolabeling of a *L. elegans* mitotic metaphase cell with anti-CENH3 and anti-α-tubulin. The **inset** shows an enlarged DAPI-stained chromosome. The boundaries of the centromere groove are marked by arrows. **B** Image tilt series of the same cell showing 3 different views after rotations of the cell (**insets** show orientation). **C** Optical cross-sectioning: metaphase chromosomes after immunostaining with anti-CENH3 and anti-α-tubulin. Interaction points between centromeres and α-tubulin are indicated (arrows).

ley secondary electron (SE) detector and an in-lens SE detector. Specimens stained with Platinum Blue were examined uncoated at 5–10 kV with a semiconductor (QBSD) back-scattered electron detector. Prior to focused ion beam (FIB) milling, specimens were carbon-coated with 9 nm by electron beam gun (BAE 080T, Balzers). The FIB ion beam (Ga-emitter) was operated at 30 kV with a milling current of 5 pA. FIB sections were performed with specimen stage tilted to 54° and recorded with an electron beam voltage of 1.5 kV.

Results

Holocentric Chromosomes of L. elegans *Exhibit a Longitudinal Groove*

Mitotic chromosomes of *L. elegans* appeared to exhibit a longitudinal groove-like structure along prophase and metaphase chromosomes after DAPI staining (fig. 1, 2; online suppl. video 1; for all online suppl. material, see www.karger.com/doi/10.1159/000327713). To verify whether this structure correlates with centromeric elements, a *Luzula* CENH3-specific antibody [Nagaki et al., 2005] was applied for immunostaining. From late prophase through anaphase (fig. 1, 2; online suppl. video 1, 2), CENH3 signals of *L. elegans* appeared as pairs of parallel continuous lines and colocalized with the putative groove along each sister chromatid. The CENH3 signals appeared to be centered within the groove (fig. 1C, 2) and extended along almost the whole chromosome except for the most terminal regions (fig. 1A, B). At telophase, CENH3 signals became more diffuse (fig. 2). Unlike the situation in monocentric species, at interphase only diffuse dot-like CENH3 signals were observed (fig. 2).

SEM was performed on isolated chromosomes to investigate the holocentric chromosome structure of *L. elegans* with higher resolution. Individual chromosomes were clearly distinguishable, but it was striking that they maintained contact to each other in all mitotic stages until anaphase as previously noted [Braselton, 1971] (fig. 3). FIB milling could show that grooves were present on both lateral sides of these chromosomes (fig. 3A, B). On average, the groove was about 75% of the total chromosome length (approx. 3–5 μm) and approximately 200–400 nm wide. Sequential FIB milling showed that the depth of the groove was variable, in the range of 50–140 nm. For comparison with DAPI staining, Platinum Blue was applied

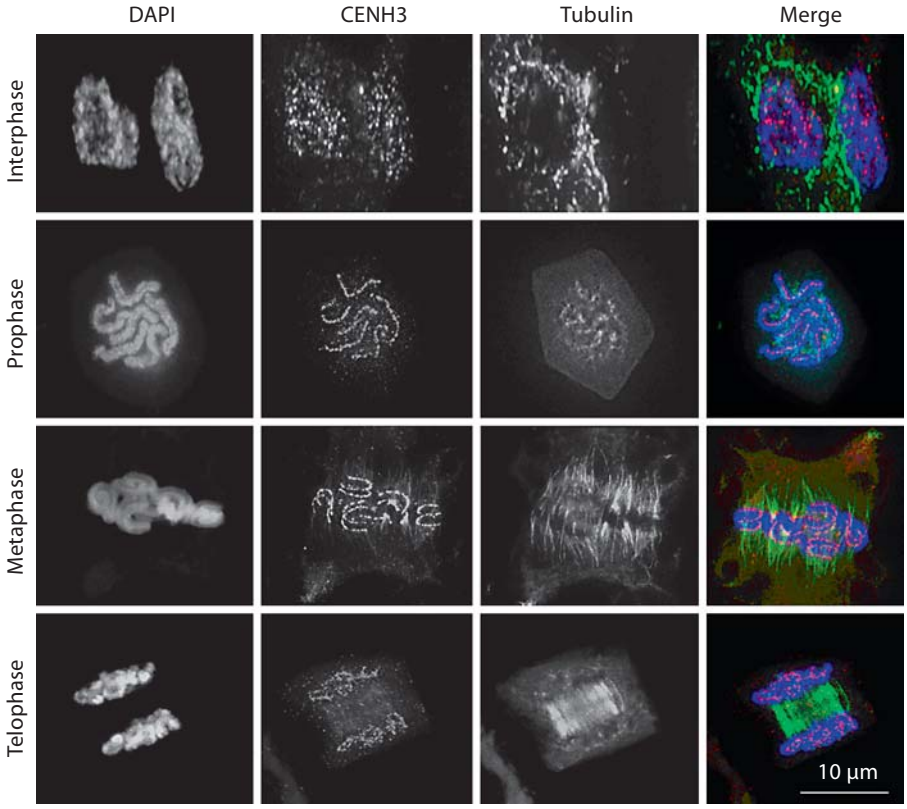

Fig. 2. Fluorescence light microscopy of *L. elegans* chromosomes at different stages of mitosis. DAPI-stained chromosomes are blue, CENH3 signals are red, and α-tubulin is green. Interphase nuclei show diffuse CENH3 foci. At prophase, chromosomes are curvy, showing tentatively continuous chains of CENH3 signals. During metaphase, chromosomes shorten and are more curved and groove along the longitudinal axis of each sister chromatid. The continuous CENH3 signal colocalizes with the groove and with microtubule ends. In telophase, chromosomes start to decondense, the CENH3 signals become diffuse and less intense, and highly organized parallel microtubules are located at the forming phragmoplast.

for SEM analysis of DNA amount and distribution (fig. 3C–F). The back-scattered electron signal showed that the DNA distribution matched chromosome topography: a much weaker Platinum Blue signal corresponded with size and shape of the groove (fig. 3D, F).

Both light microscopy and SEM investigations demonstrated a remarkably tight coalescence of sister chromatids. Optical sectioning of metaphase chromosomes with deconvolution light microscopy showed no difference in DAPI signal intensity between sister chromatids (fig. 1C); they were not distinguishable before completion of anaphase. In both Platinum Blue analysis in SEM and physical sectioning with FIB/FESEM, no structural evidence defining sister chromatids at metaphase was observed (fig. 3).

Behavior of Holocentric Chromosomes at Metaphase/Anaphase Transition

As previously shown for *L. luzuloides* [Madej, 1998], the polar regions of the microtubule spindle were not well defined, and the width of the spindle was broader than its interpolar length (fig. 2). Fluorescent immunostaining of α-tubulin showed that microtubuli attachment concurred with CENH3 loci and the groove. At metaphase/anaphase transition the microtubules attached to CENH3 along both holocentric axes and were evenly distributed toward either pole so that whole chromatids moved apart in parallel (fig. 2), not forming the classical V-shape characteristic of monocentric chromosomes. From the top view (with respect to metaphase plate), chromosomes at the metaphase/anaphase transition appeared rod-like (fig. 4A), whereas from the side view they occurred mainly curved and appeared sickle-shaped (fig. 2, 4C). CENH3 signals appeared U-shaped due to 3D perspective of the chromosome curvature (fig. 2, 4; online suppl. video 2). Curvature of chromosomes at metaphase/anaphase transition going along with U-shaped CENH3 signals was also observed for the chromosomes of *L. luzuloides* (online suppl. fig. 1). During telophase, chromatids decondensed, and CENH3 appeared to exhibit a decreased signal intensity (fig. 2). The region between separated telophase chromosomes was filled with a large number of long microtubules, and phragmoplast formation occurred (fig. 2).

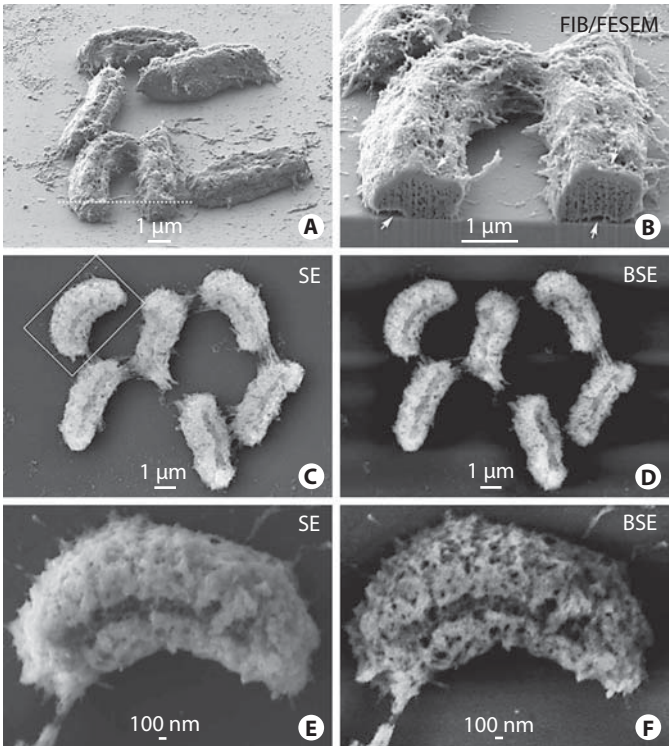

Fig. 3. Scanning electron micrographs of isolated metaphase *L. elegans* holocentric chromosomes. **A** FIB/FESEM image showing that metaphase chromosomes occur both rod-like and curved and exhibit a distinct longitudinal groove. **B** Cross-section of chromosomes (milling plane: dotted line in **A**) shows that a shallow groove is present on both sides of each chromosome (reciprocal arrows). **C–F** SEM micrograph pairs of *L. elegans* holocentric metaphase chromosomes (uncoated) showing topography with secondary electron (SE) signal and specific DNA contrasting with Platinum Blue via back-scattered electron (BSE) signals. The Platinum Blue signals are weak in the area corresponding to the size and shape of the groove due to reduced chromatin volume. **E**, **F** Detail of chromosome framed in (**C**). Images were recorded at 10 kV with an in-lens SE and a semiconductor (QBSD) backscattered electron detector.

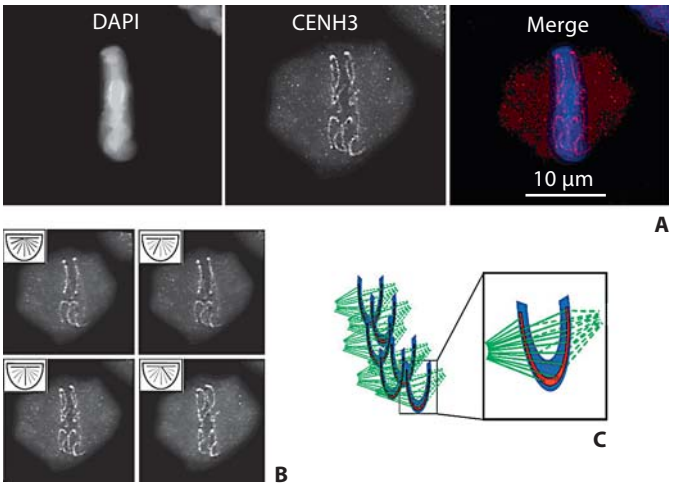

Fig. 4. Chromosome morphology at metaphase/anaphase transition of *L. elegans*. DAPI-stained chromosomes are blue and CENH3 signals are red. **A** At metaphase/anaphase transition, chromosomes are oriented in a tight planar configuration; from a top view (with respect to metaphase plate) chromosomes are not distinguishable from each other. **B** Image tilt series of the curved linear CENH3 signal of the same cell showing 4 different views after rotations of the cell (**insets** show orientation). Note the symmetry of the CENH3 signal pairs proving localization on both sister chromatids. **C** Schematic model of chromosome bending during metaphase/anaphase transition. DNA is shown in blue, CENH3 in red, and α-tubulin fibers in green.

45S rDNA Locates at one Chromosome End Distal to Centromeric Sites

The 45S rDNA probe used in this investigation hybridized to one terminal chromosome position of 1 of the 3 chromosome pairs (fig. 5A, B), and the signals appeared to cover the whole terminal end of the labeled chromosomes (fig. 5A, B). In corresponding DAPI images no secondary constriction was observed. *Arabidopsis*-type telomere-specific signals were detected on the subterminal ends of all chromosomes (fig. 5A). Terminal 45S rDNA localization was also found in *L. luzuloides* (online suppl. fig. 2A, B). As previously shown for the holocentric species *L. luzuloides* [Fuchs et al., 1995] and *Rhynchospora tenuis* [Vanzela et al., 2003], interstitial telomeric DNA sites were found (online suppl. fig. 2B) but no interstitial telomeric DNA sites were found in *L. elegans*. Surprisingly, DAPI-positive regions and 45S rDNA sites were localized distal to the telomeric sites (fig. 5A, B; online suppl. fig. 2), thereby indicating that both *L. elegans* and *L. luzuloides* host a terminal NOR. Hence, in both *Luzula* species the nucleolus-organizing region appears to 'cap' one chromosome end distal to the centromere and telomere repeats (fig. 5C; suppl. fig. 2).

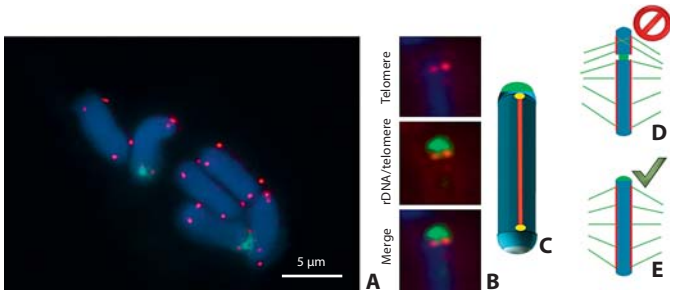

Fig. 5. A Mitotic *L. elegans* chromosomes at metaphase after fluorescence in situ hybridization with 45S rDNA (green) and *Arabidopsis*-type telomere probes (red). **B** Close-up of a 45S rDNA-carrying chromosome at (pro-)metaphase. **C** Structural model of the 45S rDNA-carrying mitotic metaphase chromosome (blue). 45S rDNA (green) forms a cup-like structure being telomere- (yellow) and centromere-free (red) and builds up the morphological chromosomal end. **D**, **E** Schematic representation of 2 possibilities for 45S rDNA location (green) in a holocentric chromosome and the resulting interaction with microtubule spindle fibers. **D** Interstitial NOR-position would generate a di-holocentric chromosome. If spindle fibers tether on both active holokinetic sites flanking the NOR pulling them to opposite poles, chromosome breaks could occur. **E** A distal NOR-position could exclude the possible negative effect of an interstitial NOR on centromere function and chromosome stability.

Discussion

Luzula elegans *Displays a Holocentric Constriction-Like Groove*

All species of the genus *Luzula* have holocentric chromosomes. However, *L. elegans* differs from other *Luzula* species in several aspects. It has fewer chromosomes (2n = 6), larger chromosomes, and exhibits a distinct longitudinal centromere groove, for which evidence is presented here. Assuming that a distinct centromeric groove is most pronounced in *L. elegans* due to the large size of the chromosomes, it is possible that the holocentric groove is a structural accommodation for the stability of these relatively large chromosomes during mitosis. A centromeric groove was less defined in *L. nivea* with smaller chromosomes [Nagaki et al., 2005] but not detectable in *L. luzuloides* (online suppl. fig. 1). Further high-resolution investigations with different organisms will shed light on whether the holocentric groove is a more or less common occurrence.

The formation of a distinct longitudinal centromeric groove in *L. elegans* could be based on a different conformation of CENH3-containing nucleosomes compared to canonical histone H3-containing ones. This is based on unique physical properties conferred by the CENP-A centromere targeting domain [Black et al. 2004], a part of the C-terminal histone fold domain of CENP-A essential for its centromeric localization [Sullivan et al., 1994; Black et al., 2007a], including for instance a conformationally rigidified interface [Black et al., 2007b; Sekulic et al., 2010], and a compaction of the maximal dimension of CENP-A-containing compared to H3-containing heterotetramers [Sekulic et al., 2010]. Likewise, specific interactions of CENH3-containing chromatin with kinetochore proteins such as CENP-B or CENP-N [Carroll et al., 2009], which are required for kinetochore assembly and/or the interaction with spindle fibers, may also account for the distinct groove-structure.

Early electron microscopic studies showed interstitial kinetochore regions on holocentric chromosomes of *L. purpurea* (renamed *L. elegans*), which indicated that holocentric kinetochores are not distributed diffusely along the chromosomes, but rather are distinct sites along the poleward chromosome surface [Braselton, 1971]. These interstitial kinetochore regions are reflected in our observation of a cell-cycle-dependent CENH3 pattern. CENH3 formed diffuse small dot-like foci in interphase, became more ordered and concentrated in prophase to early prometaphase, and merged to a tentative continuous line during metaphase when chromosomes were maximally condensed (fig. 1, 2). Modulation of CENH3 signals from weak foci to an almost continuous signal from prophase to metaphase was also reported for *L. nivea* [Nagaki et al., 2005].

Bending of Chromosomes during Metaphase/Anaphase Transition

In most of the literature, holocentric chromosomes are generally described to be stable in shape during mitosis forming rod-shape structures [for review see Dernburg, 2001; Viera et al., 2009]. Our light microscopic analysis clearly revealed a curvature of large mitotic chromosomes of *L. elegans* resulting in a sickle shape at metaphase/anaphase transition. We hypothesize that the sickle shape of mitotic chromosomes could be explained by the pulling forces of microtubule bundles along the entire length of centromeres towards corresponding microtubule organizing centers. Assuming an almost equal length and equal pulling forces of microtubules, the length of the attachment region would dictate the chromosome bending process (fig. 2, 4). Likewise, equal microtubule length would allow simultaneous separation of sister chromatids at the onset of anaphase, causing centromere sites to reach the spindle poles almost simultaneously at telophase. This constraint would also

explain the reduced oscillation frequency and reduced amplitude of aligned metaphase chromosomes compared to monocentrics [for review see Maddox et al., 2004] and may be a reason for the constant distance of sister kinetochores observed along the length of other holocentric chromosomes [Desai et al., 2003; Maddox et al., 2004]. Notably, in preparations of mitotic *L. elegans* cells fixed with ethanol:acetic acid for SEM and FISH, sickle-shaped chromosomes were less pronounced. This could be due to the disruption of spindle assembly during fixation and supports the assumption of the involvement of microtubule-based forces leading to chromosome curvature. Unlike those for monocentric chromosomes of similar size [e.g., barley; Houben et al., 2007], for *L. elegans* the polar regions of the microtubule spindle at metaphase/anaphase transition were more extended (fig. 2). Hence, the microtubule-organizing centers seem to occupy a larger region than known for monocentric species.

The forces determining the chromosome bending process would be less influential for species with holocentric chromosomes of shorter length. It would be expected that small chromosomes are less likely to curve due to their relatively higher flexural strength. However, even *Luzula* species with shorter chromosomes like *L. luzuloides* exhibit chromosome curvature during metaphase/anaphase transition (online suppl. fig. 1). In addition, a change of the chromosome shape at metaphase/anaphase transition has been noted also for the holocentric species *Oncopeltus fasciatus* [Comings and Okada, 1972], *Rhynchospora tenuis* [Guerra et al., 2010], and mites [Wrensch et al., 1994]. It appears that bending at metaphase is a common, but not mandatory, occurrence for holocentric chromosomes.

Does Holocentricity Dictate a Terminal Position of NOR Sites?

It is striking that the longitudinal centromeric groove in *L. elegans* does not extend along the entire chromatid, but discontinues at each subterminal end.

The 45S rDNA of *L. elegans* exhibits a terminal NOR located at the distal centromere-free tip of one of the chromosome pairs. Notably, high-resolution FISH on super-stretched barley chromosomes revealed also DAPI-positive chromosome termini distal to telomeric repeats [Valarik et al., 2004]. Although the NOR appears to 'cap' the chromosome in *L. elegans* and also *L. luzuloides*, it is unlikely that the rDNA is located at the physical end of the chromosomal DNA strand. Rather, a 45S rDNA-containing chromatin protrusion might mimic the morphological end of the chromosome. However, no distinct structure associated with terminal NORs was observed [Schroeder-Reiter et al., 2006]. A centromere-free distal end of holocentric chromosomes was also demonstrated for *C. elegans* [Moore et al., 1999], *L. nivea* [Nagaki et al., 2005], and the insect *Oncopeltus fasciatus* [Comings and Okada, 1972].

Our findings are consistent with previous reports on the position of the 45S rDNA in many holocentric species. For example, in plants a terminal distribution of 45S rDNA was found in 23 species of *Eleocharis* (Cyperaceae) [da Silva et al., 2010], in 8 species of *Rhynchospora* (Cyperaceae) [Vanzela et al., 1998], and in the holoparasite *Cuscuta approximata* [Guerra and Garcia, 2004]. Strikingly, the terminal position of 45S rDNA was maintained in spite of the occurrence of multiple translocations [da Silva et al. 2010]. Also many animals with holocentric chromosomes, for example the aphids *Acyrthosiphon pisum* [Bizzaro et al., 2000] and *Schizaphis graminum* [Mandrioli et al., 1999], the scorpion *Tityus bahiensis* [Schneider et al., 2009], the codling moth *Cydia pomonella* [Fukova et al., 2005], and the nematode *C. elegans* [Albertson, 1984], are characterized by terminal NOR-positions. Holocentric heteropterans seem to be an exception because they possess terminal and non-terminal 45S rDNA sites [Papeschi et al., 2003; Cattani and Papeschi, 2004; Rebagliati and Mola, 2010]. However, the distribution of CENH3 in holocentric species possessing chromosomes with interstitial 45S rDNA sites remains to be studied.

This provokes the question whether a functional interrelationship exists between holocentricity and a distal NOR position. The NOR is a docking site for nucleolar proteins involved in nucleolus formation and transcription of 45S rDNA. Late condensation of the NOR region with respect to the rest of the chromosomes is possibly the result of the late retention of the nucleolus [Raska et al., 2004]. SEM investigations have shown that NORs can be indeed structurally different from surrounding chromatin: interstitial constrictions are characterized by parallel fibrils with sparse DNA distribution [Wanner and Formanek, 1995]. This distinct chromatin structure might interfere with the formation and function of centromeres in holokinetic chromosomes. In case of an interstitial NOR position, a mutual exclusion of NOR and centromere position would generate a dicentric chromosome (fig. 5D). If the centromeres on both sites of the NOR region remained active, a di-holocentric chromosome would be doubly tethered in case of a twist between sister chromatids within the less con-

densed NOR and could be pulled to the opposite poles of the spindle when the cell divides, causing chromosome breaks (fig. 5D). Hence, it is plausible to speculate that the position of active 45S rDNA clusters in distal centromere-free regions (fig. 5E) could be required to ensure chromosome stability.

Acknowledgements

We are grateful to Ingo Schubert for fruitful discussion. Also, we appreciate excellent technical assistance by Sabine Steiner and Claudia Bubenzer-Hange. This work was supported by the IPK (Gatersleben), the Leibniz Association (WGL), the Deutsche Forschungsgemeinschaft (DFG), and the LMU Mentoring Program.

References

Albertson DG: Localization of the ribosomal genes in *Caenorhabditis elegans* chromosomes by in situ hybridization using biotin-labeled probes. EMBO J 3:1227–1234 (1984).

Albertson DG, Thomson JN: The kinetochores of *Caenorhabditis elegans*. Chromosoma 86: 409–428 (1982).

Allshire RC, Karpen GH: Epigenetic regulation of centromeric chromatin: old dogs, new tricks? Nat Rev Genet 9:923–937 (2008).

Bizzaro D, Mandrioli M, Zanotti M, Giusti M, Manicardi GC: Chromosome analysis and molecular characterization of highly repeated DNAs in the aphid *Acyrthosiphon pisum* (Aphididae, Hemiptera). Genetica 108:197–202 (2000).

Black BE, Foltz DR, Chakravarthy S, Luger K, Woods VL Jr, Cleveland DW: Structural determinants for generating centromeric chromatin. Nature 430:578–582 (2004).

Black BE, Jansen LE, Maddox PS, Foltz DR, Desai AB, et al: Centromere identity maintained by nucleosomes assembled with histone H3 containing the CENP-A targeting domain. Mol Cell 25:309–322 (2007a).

Black BE, Brock MA, Bedard S, Woods VL Jr, Cleveland DW: An epigenetic mark generated by the incorporation of CENP-A into centromeric nucleosomes. Proc Nat Acad Sci USA 104:5008–5013 (2007b).

Braselton JP: The ultrastructure of the non-localized kinetochores of *Luzula* and *Cyperus*. Chromosoma 36:89–99 (1971).

Buchwitz BJ, Ahmad K, Moore LL, Roth MB, Henikoff S: A histone-H3-like protein in *C. elegans*. Nature 401:547–548 (1999).

Carroll CW, Silva MCC, Godek KM, Jansen LET, Straight AF: Centromere assembly requires the direct recognition of CENP-A nucleosomes by CENP-N. Nat Cell Biol 11:896–902 (2009).

Cattani MV, Papeschi AG: Nucleolus organizing regions and semi-persistent nucleolus during meiosis in *Spartocera fusca* (Thunberg) (Coreidae, Heteroptera). Hereditas 140:105–111 (2004).

Comings DE, Okada TA: Holocentric chromosomes in *Oncopeltus*: kinetochore plates are present in mitosis but absent in meiosis. Chromosoma 37:177–192 (1972).

Cox AV, Bennett ST, Parokonny AS, Kenton A, Callimassia MA, Bennett MD: Comparison of plant telomere locations using a PCR-generated synthetic probe. Ann Bot 72:239–247 (1993).

da Silva CR, Quintas CC, Vanzela AL: Distribution of 45S and 5S rDNA sites in 23 species of *Eleocharis* (Cyperaceae). Genetica 138:951–957 (2010).

Dernburg AF: Here, there, and everywhere: kinetochore function on holocentric chromosomes. J Cell Biol 153:33–38 (2001).

Desai A, Rybina S, Müller-Reichert T, Shevchenko A, Shevchenko A, et al: KNL-1 directs assembly of the microtubule-binding interface of the kinetochore in *C. elegans*. Genes Dev 17:2421–2435 (2003).

Earnshaw WC, Rothfield N: Identification of a family of human centromere proteins using autoimmune sera from patients with scleroderma. Chromosoma 91:313–321 (1985).

Fuchs J, Brandes A, Schubert I: Telomere sequence localization and karyotype evolution in higher plants. Plant Syst Evol 196:227–241 (1995).

Fukova I, Nguyen P, Marec F: Codling moth cytogenetics: karyotype, chromosomal location of rDNA, and molecular differentiation of sex chromosomes. Genome 48:1083–1092 (2005).

Gerlach WL, Bedbrook JR: Cloning and characterization of ribosomal RNA genes from wheat and barley. Nucleic Acids Res 7:1869–1885 (1979).

Guerra M, Garcia MA: Heterochromatin and rDNA sites distribution in the holocentric chromosomes of *Cuscuta approximata* Bab. (Convolvulaceae). Genome 47:134–140 (2004).

Guerra M, Cabral G, Cuacos M, González-García M, González-Sánchez M, et al: Neocentrics and holokinetics (holocentrics): chromosomes out of the centromeric rules. Cytogenet Genome Res 129:82–96 (2010).

Houben A, Schroeder-Reiter E, Nagaki K, Nasuda S, Wanner G, et al: CENH3 interacts with the centromeric retrotransposon cereba and GC-rich satellites and locates to centromeric substructures in barley. Chromosoma 116:275–283 (2007).

Howe M, McDonald KL, Albertson DG, Meyer BJ: HIM-10 is required for kinetochore structure and function on *Caenorhabditis elegans* holocentric chromosomes. J Cell Biol 153:1227–1238 (2001).

Kato A, Albert PS, Vega JM, Birchler JA: Sensitive fluorescence in situ hybridization signal detection in maize using directly labeled probes produced by high concentration DNA polymerase nick translation. Biotech Histochem 81:71–78 (2006).

Kitagawa R: Key players in chromosome segregation in *Caenorhabditis elegans*. Front Biosci 14:1529–1557 (2009).

Maddox PS, Oegema K, Desai A, Cheeseman IM: 'Holo'er than thou: chromosome segregation and kinetochore function in *C. elegans*. Chromosome Res 12:641–653 (2004).

Madej A: Spindle microtubules and chromosome behaviour in mitosis of *Luzula luzuloides*, a species with holokinetic chromosomes. Acta Biologica Cracoviensia Series Botanica 40:61–67 (1998).

Mandakova T, Lysak MA: Chromosomal phylogeny and karyotype evolution in x = 7 crucifer species (Brassicaceae). Plant Cell 20: 2559–2570 (2008).

Mandrioli M, Ganassi S, Bizzaro D, Manicardi GC: Cytogenetic analysis of the holocentric chromosomes of the aphid *Schizaphis graminum*. Hereditas 131:185–190 (1999).

Martin R, Busch W, Herrmann RG, Wanner G: Efficient preparation of plant chromosomes for high-resolution scanning electron microscopy. Chromosome Res 2:411–415 (1994).

Moore LL, Morrison M, Roth MB: HCP-1, a protein involved in chromosome segregation, is localized to the centromere of mitotic chromosomes in *Caenorhabditis elegans*. J Cell Biol 147:471–480 (1999).

Nagaki K, Kashihara K, Murata M: Visualization of diffuse centromeres with centromere-specific histone H3 in the holocentric plant *Luzula nivea*. Plant Cell 17:1886–1893 (2005).

Oegema K, Hyman AA: Cell division, in WormBook (ed): The *C. elegans* Research Community, pp 1–40 (2006) http://www.wormbook.org.

Papeschi AG, Mola LM, Bressa MJ, Greizerstein EJ, Lia V, Poggio L: Behaviour of ring bivalents in holokinetic systems: alternative sites of spindle attachment in *Pachylis argentinus* and *Nezara viridula* (Heteroptera). Chromosome Res 11:725–733 (2003).

Pimpinelli S, Goday C: Unusual kinetochores and chromatin diminution in *Parascaris*. Trends Genet 5:310–315 (1989).

Raska I, Koberna K, Malinsky J, Fidlerova H, Masata M: The nucleolus and transcription of ribosomal genes. Biol Cell 96:579–594 (2004).

Rebagliati PJ, Mola LM: Meiotic behavior and karyotypic variation in *Acledra* (Pentatomidae, Heteroptera). Genet Mol Res 9:739–749 (2010).

Schneider MC, Zacaro AA, Pinto-da-Rocha R, Candido DM, Cella DM: Complex meiotic configuration of the holocentric chromosomes: the intriguing case of the scorpion *Tityus bahiensis*. Chromosome Res 17:883–898 (2009).

Schroeder-Reiter E, Houben A, Grau J, Wanner G: Characterization of a peg-like terminal NOR structure with light microscopy and high-resolution scanning electron microscopy. Chromosoma 115:50–59 (2006).

Sekulic N, Basset EA, Rogers DJ, Black BE: The structure of $(CENP\text{-}A\text{-}H4)_2$ reveals physical features that mark centromeres. Nature 467: 347–351 (2010).

Sullivan KF, Hechenberger M, Masri K: Human CENP-A contains a histone H3 related histone fold domain that is required for targeting to the centromere. J Cell Biol 127:581–592 (1994).

Vanzela ALL, Cuadrado A, Jouve N, Luceno M, Guerra M: Multiple locations of the rDNA sites in holocentric chromosomes of *Rhynchospora* (Cyperaceae). Chromosome Res 6: 345–349 (1998).

Vanzela ALL, Cuadrado A, Guerra M: Localization of 45S rDNA and telomeric sites on holocentric chromosomes of *Rhynchospora tenuis* Link (Cyperaceae). Genet Mol Biol 26: 199–201 (2003).

Valarik M, Bartos J, Kovarova P, Kubalakova M, de Jong JH, Dolezel J: High-resolution FISH on stretched flow-sorted plant chromosomes. Plant J 37:940–950 (2004).

Viera A, Page J, Rufas JS: Inverted meiosis: the true bugs as a model to study. Genome Dyn 5:137–156 (2009).

Wanner G, Formanek H: Imaging of DNA in human and plant chromosomes by high-resolution scanning electron microscopy. Chromosome Res 3:368–374 (1995).

Wrensch DL, Kethley JB, Norton RA: Cytogenetics of holokinetic chromosomes and inverted meiosis: keys to evolutionary success of mites, with generalization on eukaryotes, in Houck MA (ed): Mites – Ecological and Evolutionary Analyses of Life-History Patterns, pp 282–343 (Chapman & Hall, New York 1994).